



DEVELOPMENT OF A ROTATING SOURCE LOCALISATION TECHNIQUE BASED ON CYCLOSTATIONARY TIME-FREQUENCY ANALYSIS

Maximilian Behn and Ulf Tapken

German Aerospace Center (DLR), Institute of Propulsion Technology, Engine Acoustics Department
Müller-Breslau-Str. 8, 10623 Berlin, Germany

Abstract

A new approach for sound source localisation of rotating and static sources is presented, which adopts a hybrid time-frequency analysis in order to facilitate simultaneous detection of both types of sources. The analysis technique makes use of the assumption of cyclostationarity enabling the calculation of instantaneous spectra, i.e. a sound pressure spectrum at each angular position along the trajectory of the rotating sources. Adaptations of Compressed Sensing-based and DAMAS deconvolution algorithms to the framework of simultaneous sparse approximation are introduced. The results for simulated test cases comprising tonal and broadband source spectra show the capabilities of the localisation technique in comparison with reference Beamforming techniques. As this is an ongoing development further advancements are discussed.

Nomenclature

$\mathbf{q}_{inst}(\varphi_{rot})$	Source strength in Pa	\mathbf{D}	De-Dopplerisation matrix
\mathbf{F}	Fourier deconvolution matrix	$\mathbf{G}_{inst}(\varphi_{rot})$	Combined steering matrix
$\mathbf{G}_{rot}(\varphi_{rot})$	Steering matrix, rotating sources	\mathbf{G}_{fix}	Steering matrix, static sources
$\mathbf{H}_{inst,PSF}(\varphi_{rot})$	Point Spread Function	$\mathbf{p}_{inst,fix}(\varphi_{rot})$	Spectrum, static sources in Pa
$\mathbf{p}_{inst}(\varphi_{rot})$	Combined spectrum in Pa	$\mathbf{p}_{inst,rot}(\varphi_{rot})$	Spectrum, rotating sources in Pa
\mathbf{p}_{VRA}	Complex sound pressure, virtual rotating array in Pa	$\mathbf{S}_{pp,inst}(\varphi_{rot})$	Instantaneous CSM in Pa ²
		\mathbf{W}_{AMA}	Matrix for azimuthal mode decomposition

f	Analysis frequency in Hz	f_{rot}	Rotor speed in Hz
m	Azimuthal mode order	N_{mic}	Number of microphones
$N_{sources}$	Number of sources	$N_{samples}$	Number of samples per block
$p(t)$	Raw microphone signal in Pa	$\tilde{p}(\varphi_{rot})$	Resampled signal in Pa
$\tilde{p}_a(\varphi_{rot})$	Analytic signal in Pa	$H[\cdot]$	Hilbert transform
φ_{rot}	Angular rotor position in rad	$\text{diag}(\cdot)$	Matrix diagonal extraction
$\ \cdot\ _F$	Frobenius matrix norm		
CSM	Cross-spectral matrix		
S-DAMAS	Simultaneous deconvolution approach for the mapping of acoustic sources		
DCS	Distributed Compressed Sensing		
NNLS	Non-negative least squares		
SOMP	Simultaneous Orthogonal Matching Pursuit		
SSA	Simultaneous Sparse Approximation		

1 Introduction

The characterisation of sound source distributions at the rotor of e.g. turbo fans, wind turbines and ventilators has gained importance to support the development of noise reduction technologies. Microphone array methods have been developed to localise rotating, spatially distributed sources in time domain [22] and frequency domain [10, 15, 18, 23]. Hybrid techniques make use of e.g. interpolation to the rotating frame of reference in order to obtain the signals of a virtual rotating array [8, 13] with subsequent analysis in frequency domain. Chen & Huang [7] applied Wavelet-based beamforming to achieve a time-frequency analysis of the sound field radiated from rotating sources. In Ref. [16], a deconvolution approach for sources in different motion modes is described, which makes use of point spread functions for the respective sources with respect to the different motion modes, i.e. the point spread of a rotating source in a fixed frame of reference.

Common to all techniques presented previously is the lack of simultaneous separation capabilities in the presence of rotating and static sources. This scenario occurs for the investigation of sound generation mechanisms at rotor-stator stages. As part of an ongoing research on the sound generation effects due to inflow distortion a new localisation method is under development based on cyclostationary time-frequency analysis with three main goals:

1. simultaneous separation of rotating and static sources,
2. detection of coherent and incoherent sources,
3. identification of rotor-dependent amplitude modulation of the sources.

The first goal is motivated by the observed shortcomings of existing techniques, where the presence of sources, which are out-of-focus (static sources for rotating focus and vice versa), leads to smearing effects in the resulting source maps. If these out-of-focus sources are particularly strong, they have the potential to mask the sources of interest and cause the source localisation to fail.

Achieving the second goal will enable detailed analysis of the sound generation of rotor-coherent and rotor-incoherent sound field components, which are generally linked to different source mechanisms [9, 17]. The rotor-coherent components are characterised by purely periodic, tonal sound fields and related to the aerodynamic interaction of rotor and stator. The rotor-incoherent components comprise the broadband sound field components, which are generated by interaction of the rotor with inflow turbulence as well as interaction of the stator vanes with turbulence of the rotor wakes.

At last, the third goal accounts for the impact of inhomogeneous flow profiles on the sound sources. The common sound generation mechanisms related to the blade thickness, lift and drag are affected and additional source mechanisms occur, which can lead to increased sound radiation. The periodical motion of the rotor evokes a modulation of the sound generation depending on the spatial structure of the inhomogeneous flow profile [24]. For the analysis of the resulting periodically modulated sound field the Wigner-Ville spectrum is a useful tool [1].

The current study presents the filtering of signal components relating to static and rotating sources, from which instantaneous spectra are determined. The instantaneous spectra serve as input to deconvolution algorithms that enable simultaneous detection of static and rotating sources for tonal and broadband source spectra, respectively. An assessment of the new localisation technique in terms of detected source positions and strengths is performed on the basis of simulated test cases. The application of Wigner-Ville analysis is out of the scope of the present paper.

2 Filtering components from rotating and static sources

Stator- and rotor-bound sources in turbomachinery stages radiate sound simultaneously, which is then measured by a microphone array. For source localisation it is required to filter the signal components that relate to the respective sources at the considered analysis frequency. In the following, a hybrid time-frequency technique is described that allows filtering signal components from rotating and static sound sources.

First, the microphone signals $p(t)$ are resampled using the rotor shaft trigger signal, so that a fixed phase reference is established and the microphone signals are given with respect to the azimuthal rotor position φ_{rot} as $\tilde{p}(\varphi_{rot})$. Next, it is essential to use the analytic signal in order to avoid undesirable interference effects [5]:

$$\tilde{p}_a(\varphi_{rot}) = \tilde{p}(\varphi_{rot}) + i \cdot H[\tilde{p}(\varphi_{rot})], \quad (1)$$

with $\tilde{p}_a(\varphi_{rot})$ the analytic signal associated with the real-valued microphone signal $\tilde{p}(\varphi_{rot})$ and the Hilbert transform $H[\cdot]$. The spectrum of the analytic signal only comprises positive frequencies and hence, is complex-valued.

In order to analyse rotating and static sound sources, a decomposition of the sound pressure signal into the components originating from static and rotating sources is sought, respectively. For static sources, the signal filtering is directly achieved by the discrete Fourier transform (DFT):

$$\hat{p}_a = \frac{1}{N_{samples}} \sum_{n=0}^{N_{samples}-1} \tilde{p}_a(\varphi_{rot}(n)) \cdot e^{+i \frac{f}{f_{rot}} \varphi_{rot}(n)}, \quad (2)$$

where f is the analysis frequency and f_{rot} is the rotor speed in Hz. The signal length $N_{samples}$ is chosen as an integer multiple of the number of samples per rotor revolution, so that the DFT is evaluated over a number of complete revolutions.

In order to facilitate the separation of rotating and static sources in the subsequent Beamforming analysis the use of instantaneous spectra is proposed. The instantaneous spectrum is a time-frequency representation of a signal, where the complex Fourier amplitude is given at every moment in time resp. at every azimuthal rotor position. In case of static sources, the instantaneous spectra is calculated from the complex pressure matrix \mathbf{p}_a with dimensions $N_{mic} \times N_{samples}$ as follows:

$$\mathbf{p}_{inst,fix} = \mathbf{p}_a \cdot \mathbf{F} \cdot \frac{\mathbf{1}}{N_{samples}}, \quad (3)$$

with the Fourier deconvolution matrix $\mathbf{F} = \text{diag} \left(e^{+i \frac{f}{f_{rot}} \varphi_{rot}(0)}, \dots, e^{+i \frac{f}{f_{rot}} \varphi_{rot}(N_{samples}-1)} \right)$ and the all-ones matrix $\mathbf{1}$ with dimensions $N_{samples} \times N_{samples}$.

As described by Poletti [19], the rotation of sources results in multi-component spectra due to a Doppler effect. The frequency shifts are proportional to the azimuthal mode order occurring in the spatial Fourier decomposition of the radiated sound field (see eq. (10)):

$$f_m = f - m f_{rot}. \quad (4)$$

A typical approach for de-Dopplerisation is to roll back the frequency shifts $m \cdot (2\pi f_{rot})$ in the azimuthal mode domain [15], which requires the use of microphone ring arrays. The computation of instantaneous spectra for rotating sources is performed by the following procedure applied to a pressure matrix \mathbf{p}_a composed for a microphone ring:

1. spatial Fourier decomposition into azimuthal modes,
2. deconvolution with analysis frequency component,
3. de-Dopplerisation with respect to mode order,
4. averaging,
5. application of mode-dependent Doppler shifts for signal synthesis,
6. inverse spatial Fourier decomposition into spatial domain, i.e. individual microphone spectra.

A compact formulation is found by use of two different matrix products, the standard matrix product $\mathbf{A}\mathbf{B}$ and the Hadamard (elementwise) matrix product $\mathbf{A} \circ \mathbf{B}$:

$$\mathbf{p}_{inst,rot} = \mathbf{W}_{AMA} \left(\mathbf{D}^* \circ \left(\left(\mathbf{D} \circ \left(\frac{1}{N_{mic}} \mathbf{W}_{AMA}^H \mathbf{p}_a \mathbf{F} \right) \right) \frac{\mathbf{1}}{N_{samples}} \right) \right). \quad (5)$$

Here, \mathbf{W}_{AMA} denotes the matrix of mode transfer function for a ring array $e^{im\varphi}$ (cp. [3]), where $m = 0$ is omitted, because this component is not affected by the Doppler effect and already included in $\mathbf{p}_{inst,fix}$. \mathbf{D} is the de-Dopplerisation matrix with entries $e^{im\varphi_{rot}(n)}$. The matrix operators $[\dots]^H$ and $[\dots]^*$ are the hermitian matrix and complex conjugate matrix, respectively. Note that

the formulation in eq. (5) is only valid for ring arrays with uniform sensor spacing. In case of irregular ring arrays, the azimuthal mode analysis at step 1 has to be performed separately using e.g. Compressed Sensing-based mode analysis [3].¹

The filtered sound field components $\mathbf{p}_{inst,fix}$ and $\mathbf{p}_{inst,rot}$ have to be analysed simultaneously, since the signal component relating to $m = 0$ cannot be assigned unambiguously to the rotating or static source components. For this reason, the sum of both components is used in the following and called the instantaneous spectrum for simplicity:

$$\mathbf{p}_{inst} := \mathbf{p}_{inst,fix} + \mathbf{p}_{inst,rot}. \quad (6)$$

Under the assumption that the sound sources of a turbomachinery stage are related to the rotor revolution and that the statistical quantities such as correlations are periodic with the rotor cycle duration $T_{rot} = 1/f_{rot}$, the sound field can be modeled as cyclostationary [1, 4]. As a result, an instantaneous cross-spectral matrix (CSM) of the filtered sound pressure components $\mathbf{S}_{pp,inst}(\varphi_{rot}(n))$ is obtained by averaging the instantaneous spectra for each rotor position $\varphi_{rot}(n)$ separately:

$$\mathbf{S}_{pp,inst}(\varphi_{rot}(n)) = \langle \mathbf{p}_{inst}(\varphi_{rot}(n)), \mathbf{p}_{inst}^H(\varphi_{rot}(n)) \rangle. \quad (7)$$

3 Simultaneous determination of source strengths

The identification of source positions and amplitudes is performed by use of matrix inversion techniques, such as Compressed Sensing techniques (e.g. [3]) and DAMAS deconvolution [6]. These techniques require that the steering matrix is non-singular. The instantaneous steering matrix is composed by the steering matrices of static and rotating sources:

$$\mathbf{G}_{inst}(\varphi_{rot}(n)) = [\mathbf{G}_{stat} \mid \mathbf{G}_{rot}(\varphi_{rot}(n))], \quad (8)$$

where \mathbf{G}_{stat} contains the Green functions of the static sources and $\mathbf{G}_{rot}(\varphi_{rot}(n))$ contains the Green functions of the rotating sources along their trajectory. Note that in this study the steering vector formulation IV according to Sarradj [20] is applied for normalisation.

The free-space Green function for a point source at $\vec{r}_s(t) = [r_s, \vartheta_s, \varphi_s(t)]$ is expressed as [19]:

$$p_G(\vec{r}, \vec{r}_s(t), \omega_{rot}, \omega, t) = \frac{e^{ik|\vec{r}-\vec{r}_s(t)|}}{4\pi|\vec{r}-\vec{r}_s(t)|} e^{-i\omega t} \quad (9)$$

$$= ie^{-i\omega t} \sum_{n=0}^{\infty} \sum_{m=-n}^n k_m j_n(k_m r_{<}) h_n^{(1)}(k_m r_{>}) Y_n^m(\vartheta, \varphi) \cdot Y_n^m(\vartheta_s, \varphi_s(t))^*. \quad (10)$$

¹An expression for the sound pressure amplitude of a virtually rotating array using Fourier-based interpolation [15] can be found in a similar way:

$$\mathbf{p}_{VRA} = \mathbf{W}_{AMA} \left(\mathbf{D} \circ \left(\frac{1}{N_{mic}} \mathbf{W}_{AMA}^H \mathbf{p}_{meas} \mathbf{F} \right) \right) \frac{[1, \dots, 1]^T}{N_{samples}},$$

with $[\dots]^T$ denoting the transpose.

Here, wave number $k_m = \omega/c - m\omega_{rot}/c$ associated with angular frequencies $\omega = 2\pi f$ and $\omega_{rot} = 2\pi f_{rot}$ is multiplied with the smaller radius $r_< = \min(r, r_s)$ for the interior field and with the larger radius $r_> = \max(r, r_s)$ for the exterior field. $j_n(\cdot)$ is the spherical Bessel function and $h_n^{(1)}(\cdot)$ is the spherical Hankel function of the first kind. The normalised spherical harmonic

$$Y_n^m(\vartheta, \varphi) = \sqrt{\frac{(2n+1)(n-|m|)!}{4\pi(n+|m|)!}} P_n^{|m|}(\cos \vartheta) e^{im\varphi} \quad (11)$$

with the associated Legendre function $P_n^m(\cdot)$ indicates the azimuthal structure of sound field in terms of azimuthal modes. For static source position $\varphi_s(t) = \varphi_{s,stat}$, it can be seen from eq. (9) that the steering matrix \mathbf{G}_{stat} is invariant with respect to the rotor position $\varphi_{rot}(n)$, because their transfer function is independent of time. The transfer function of any static source on a given source grid matches the transfer function of some rotating source at the same radial position, but with a circumferential offset, which impedes the simultaneous analysis of these two types of sources.

In the following, two procedures are presented that incorporate the motion types of the sources and enable analysis of tonal and broadband source spectra, respectively.

3.1 Analysis of tonal source spectra

With the instantaneous spectra and steering matrix in equations (6) and (8) a matrix equation is built for each rotor position $\varphi_{rot}(n)$:

$$\mathbf{q}_{inst}(\varphi_{rot}(n)) \mathbf{q}_{inst}(\varphi_{rot}(n)) = \mathbf{p}_{inst}(\varphi_{rot}(n)), \quad (12)$$

with the instantaneous source amplitude $\mathbf{q}_{inst}(\varphi_{rot}(n))$. \mathbf{q}_{inst} is a complex matrix of dimensions $N_{sources} \times N_{samples}$. As described above, the high degree of correlation between the steering matrices \mathbf{G}_{stat} and $\mathbf{G}_{rot}(\varphi_{rot}(n))$ makes it impossible to solve eq. (12) separately for each rotor position. A stable solution is achieved by applying simultaneous sparse approximation (SSA [25]) with the assumption that \mathbf{a}_{inst} has at most N_{mic} non-zero rows. Such a matrix exhibits so-called joint sparsity among its column vectors. Algorithms that exploit joint sparsity such as the SOMP-algorithm [25] (Simultaneous Orthogonal Matching Pursuit) enable a stable solution of eq. (12). Due to the fact that the steering matrix varies with $\varphi_{rot}(n)$, an extension of the SOMP-algorithm is used, the DCS-SOMP-algorithm (Distributed Compressed Sensing-SOMP) [2], which applies an individual steering matrix for each measurement, i.e. rotor position. A detailed description of the algorithm is omitted here for the sake of conciseness. Essentially, the DCS-SOMP-algorithm is an iterative algorithm, which performs the following steps at each iteration:

1. identification of the dominant source through the maximum correlation, i.e. scalar product, between the steering vectors of the individual sources and pressure vector over all $N_{samples}$ rotor angles,
2. extension of the set of identified dominant sources by newly identified source,
3. determination of amplitudes of all identified sources through a least-squares-fit for each rotor angle,

4. deconvolution of signal components related to all identified sources from the pressure matrix.

In this study, the maximum number of iterations is determined by a maximum allowed condition number of the submatrices containing the transfer functions between the identified sources and the microphones.

3.2 Analysis of broadband source spectra

In case of broadband source spectra the simultaneous sparse approximation is realised by adaptation of the well-known DAMAS problem [6]. Under the assumption that the sources are incoherent, a ’’dirty’’ source map is determined by application of conventional Beamforming at each rotor position and subsequent deconvolution with the point spread functions from each source point to all other source points. The ’’dirty’’ source map $\mathbf{q}_{inst,dirty}(\varphi_{rot}(n))$ is calculated by:

$$\mathbf{q}_{inst,dirty}(\varphi_{rot}(n)) = \frac{1}{N_{mic}^2} \text{diag}(\mathbf{G}_{inst}(\varphi_{rot}(n)) \mathbf{S}_{pp,inst}(\varphi_{rot}(n)) \mathbf{G}_{inst}^H(\varphi_{rot}(n))). \quad (13)$$

The point spread function is calculated in a similar way:

$$\mathbf{H}_{inst,PSF,i}(\varphi_{rot}(n)) = \frac{1}{N_{mic}^2} \text{diag}(\mathbf{G}_{inst,i}(\varphi_{rot}(n)) \mathbf{G}_{inst,i}^H(\varphi_{rot}(n))), \quad (14)$$

for each source position i separately. Here, the point spread function $\mathbf{H}_{inst,PSF}(\varphi_{rot}(n))$ accounts for the motion of the rotating sources in the way that it depends on the rotor position and is instantaneous as well. The simultaneous determination of rotating and static sources is achieved by solving the following deconvolution problem:

$$\begin{aligned} \underset{\mathbf{q}'_{inst} \in \mathbb{R}^{N_{sources} \times N_{samples}}}{\text{argmin}} \quad & \|\mathbf{q}_{inst,dirty}(\varphi_{rot}(n)) - \mathbf{H}_{inst,PSF}(\varphi_{rot}(n)) \mathbf{q}'_{inst}(\varphi_{rot}(n))\|_F^2 \quad \forall \varphi_{rot} \\ \text{subject to} \quad & \mathbf{q}'_{inst} \geq 0, \end{aligned} \quad (15)$$

where $\mathbf{q}'_{inst} \geq 0$ indicates that all source powers should be non-negative. The applied deconvolution scheme addresses the proposition by Herold et al. [12] that the DAMAS problem $\mathbf{q} = \mathbf{H}\mathbf{q}'$ can be efficiently solved by use a non-negative least squares (NNLS) solvers. As described by Kim & Haldar [14], the DCS-SOMP-algorithm allows the extension to a non-negative constraint on the source amplitude, which enables an efficient way for implementing simultaneous sparse approximation of the DAMAS problem (S-DAMAS). The general procedure to solve eq. (15) is equivalent to the DCS-SOMP-algorithm described above, except that the identification step evaluates the residual of eq. (15) and that the solution step uses a least-squares solver with non-negativity constraint. The maximum number of iterations is determined adaptively by evaluating the condition numbers of the submatrices, which contain the point spread functions of the identified sources.

4 Simulated test cases

The localisation technique is validated using the simulated setup of the b11 benchmark case provided by Herold [11]. The setup consists of a microphone ring array with 64 sensors and sources in free-field conditions. The distance between the source plane and microphone array is 0.5m. For the rotating sources a trigger signal is generated enabling trigger-synchronous resampling of the microphone signals. The rotation runs in clockwise direction resp. in negative circumferential direction. The rotational frequency of the source is $f_{rot} = 25$ Hz (equals 1500 rpm). The synthesis of radiated sound fields from rotating and static sources is performed in time domain.

The b11 benchmark data, which originally consists of two cases a and b, has been extended by additional test cases by the authors using the python tool Acoular [21], see Tab. 1, of which only test cases c and f related to single rotating and static sources both driven with broadband resp. tonal signals are discussed here:

Table 1: Description of applied test cases from the b11 simulated setup.

ID	Number of sources	Source characteristics	Motion mode
a	1	white noise	rotating
b	3	white noise, incoherent	rotating
c	2	white noise, incoherent	rotating + static
d	1	white noise, amplitude modulated	rotating
e	1	tone at 2000 Hz	rotating
f	2	tone at 2000 Hz	rotating + static
g	2	tone at 2000 Hz	static

The source grid is arranged in concentric circles starting from the center ($r = 0$ m, included in source grid) with radial step size $\Delta r = 2.5$ mm and a maximum radius of 0.3 m. The discretisation in circumferential direction is made with azimuthal step size $\Delta\phi = 5^\circ$. This results in 865 source position, which are considered for both source types, static and rotating, yielding 1730 independent sources in total.

The test consists of one actual source rotating at a radius of $r_{rot} = 0.25$ m and another fixed at a radius of $r_{stat} = 0.125$ m and azimuthal angle of 130° . The source positions at the trigger instant are the same for test cases c and f as illustrated in Fig. 1. The source amplitudes are given as equivalent sound pressure levels at 1 m distance. For test case f, both sources fluctuate at 2 kHz with the same source strength resulting in tonal source spectra. This test case is intended to illustrate the coupling between Doppler frequency shift and azimuthal mode order, which is the key aspect in filtering the components from static and rotating sources.

In order to verify the method for broadband signals, test data was generated consisting of two sources that radiate white noise. The source levels differ by three decibels with the static source having the lower amplitude. The following results are obtained for individual analysis frequencies and therefore, it is practical to provide the results in terms of power spectral density (PSD). For the given source levels the resulting PSD is approximately 47.2 dB for the rotating source and approximately 44.2 dB for the static source.

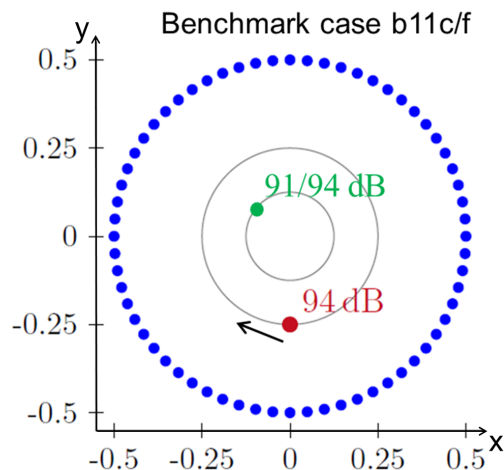


Figure 1: Illustration of the simulated setup with a single static (green) and rotating source (red) in free-field conditions for test cases b11c (broadband) and f (tonal). The rotating source has the same source strength in both test cases, but the source strength of the static source is 3 dB lower for test case b11c. The microphone positions are indicated in blue.

5 Results

5.1 Tonal source spectra

Tonal source spectra allow for a simple way to illustrate the Doppler effect for rotating sources. Figure 2a depicts the sound pressure spectrum averaged over all microphones. The source frequency is 2 kHz, but multiple tones are visible with a separation of 25 Hz, i.e. the rotational frequency f_{rot} . Comparison with the azimuthal mode spectrum proves the link between Doppler shifted frequencies and azimuthal mode order (cp. eq. (4)). At 2 kHz, several mode orders occur, which relate to the static source apart from the component with $m = 0$, where the mode spectra of both source types overlap.

In Fig. 3 the instantaneous spectrum of a single microphone is shown for test case b11f. The envelope of the instantaneous spectrum follows the envelope of the microphone signal, which has been resampled with respect to the rotor trigger. Real and imaginary part of the instantaneous spectrum vary over the rotor position periodically. The presence of the static source results in an offset of the instantaneous spectrum, because the transfer function of static sources to the microphones is constant over time. Since the source strengths are constant for this test case, the instantaneous spectrum of the static source is also constant (compare Fig. 4a).

For the source localisation using the DCS-SOMP-algorithm the maximum acceptable condition number was set to a value of 10, which was achieved for the first 14 iterations. The results of the source localisation are presented in Figs. 5 and 6. The source positions are recovered exactly by use of the DCS-SOMP-algorithm. The source levels are given over the signal block length, which comprises two complete trigger intervals, and show exact reconstruction of the source strengths. A negligible level offset occurs for the rotating sources, which is due to the approximation of the rotating Green's function by a finite series of spherical harmonics in fre-

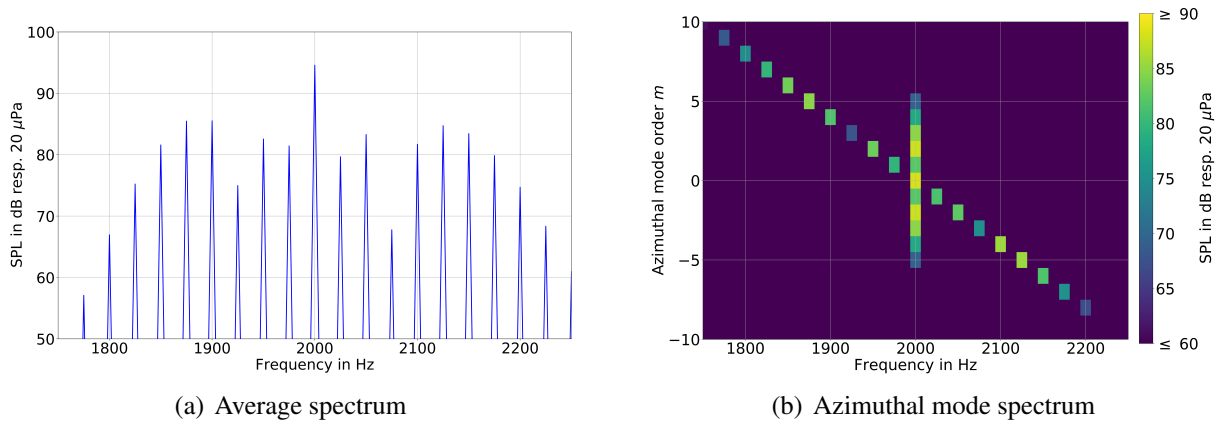


Figure 2: Spectrum averaged over all microphones and result of azimuthal mode decomposition of the microphone array data from a rotating and a static source with tonal source spectra.

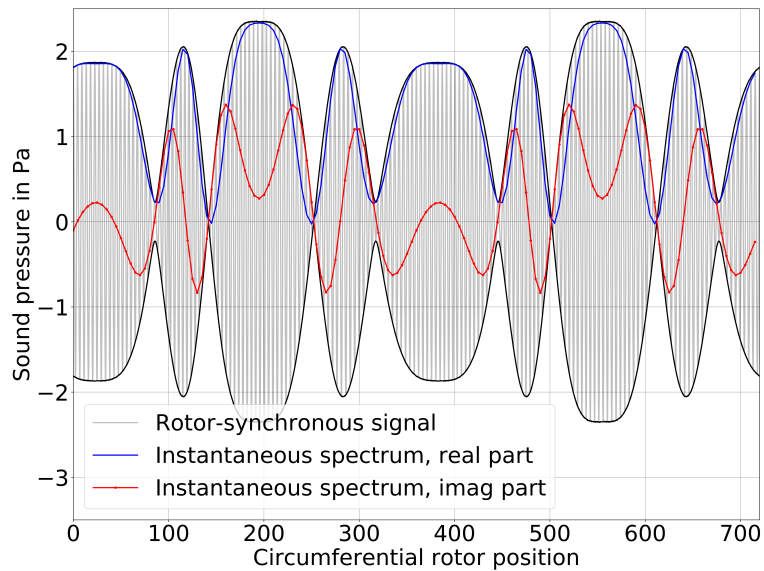


Figure 3: Instantaneous spectrum of the microphone at azimuthal angle of 0° over time, i.e. circumferential rotor position, for the 2 kHz component (test case b11f).

quency domain (cp. [19]). The trajectory of the rotating source starts at its circumferential position of 270° at the trigger instant and continues in negative azimuthal direction, i.e. from right to left in Fig. 6b. The circumferential rotor position is provided for the reconstructed amplitude of the static source in order to have the same time scale as for the rotating source. This test case proves the successful simultaneous separation and reconstruction of rotating and static sources using the proposed cyclostationary time-frequency analysis.

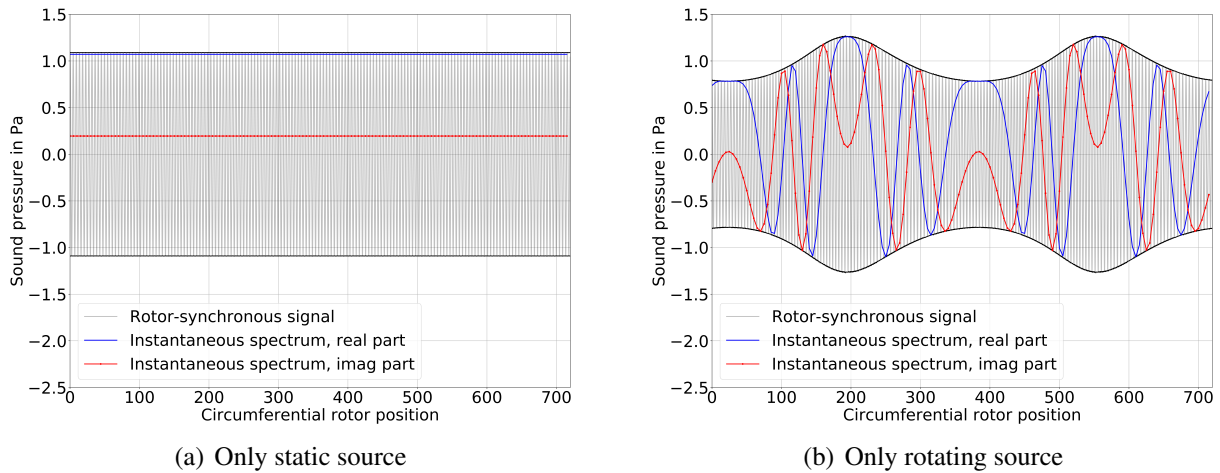


Figure 4: Instantaneous spectra of the static and rotating source separately over time, i.e. circumferential rotor position, for the 2 kHz component of the microphone at azimuthal angle of 0° .

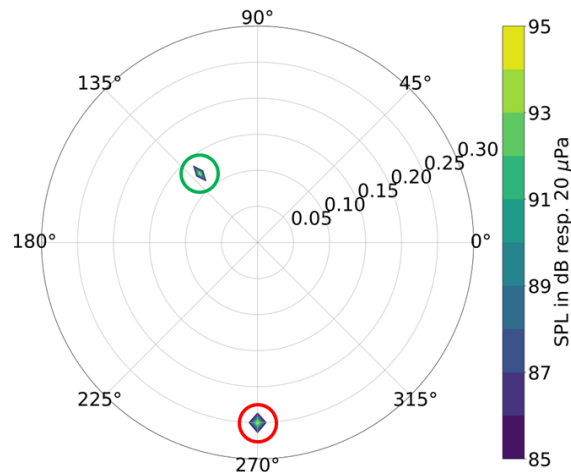


Figure 5: Source map for b11f test case evaluated at the trigger instant with analysis frequency of 2 kHz.

5.2 Broadband source spectra

The localisation of broadband sound sources is realised on the basis of instantaneous auto- and cross-spectra, which are shown exemplarily for the 2 kHz component in Fig. 7. Similar to the instantaneous spectra for tonal sound sources, the instantaneous auto- and cross-spectra are periodic with the duration between two trigger events. The presence of the static source causes an offset for the instantaneous auto- and cross-spectra in the same way as in Fig. 3.

The source localisation using S-DAMAS was performed with a chosen maximum condition number of 10, which resulted in 5 iterations for an analysis frequency of 2 kHz. The analysis was performed for analysis frequencies up to 8 kHz with similar outcome. For this reason results are presented only for 2 kHz for brevity. The results shown in Figs. 8 and 9 reveal the

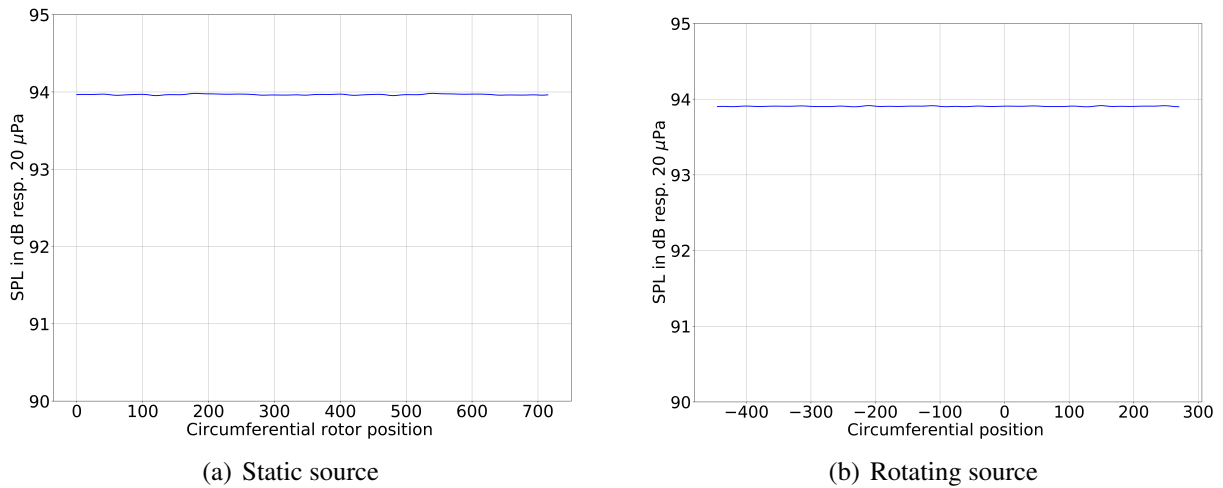


Figure 6: Instantaneous source levels at 2 kHz over two trigger intervals, i.e. two revolutions of the rotating source, for test case b11f with tonal source spectra.

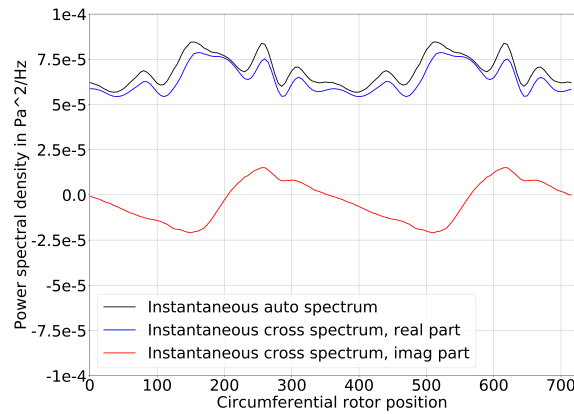


Figure 7: Instantaneous auto- and cross-spectrum of the microphone at 2 kHz and azimuthal angle of 90° and its neighbouring sensor for test case b11c.

successful identification of both sources. The amplitudes of the spurious sources in Fig. 8 range from approx. 7 to 4 dB below the actual sources. A slight overestimation of the source amplitudes by about 1 dB is observed for both types of motion. Averaging over the rotor revolution yields PSD of 48.6 dB for the rotating source and 45.5 dB for the static source, respectively, and an average level difference to spurious sources of 5 dB. Also a higher number of iterations does not increase the achievable dynamic range between the sources of interest and the spurious sources. The main reason for the overestimation of the source strengths and the limited suppression of spurious sources appears to be the high number of independent variables. At each rotor position the source strengths are determined independently, which facilitates a stronger impact of components from neighbouring frequencies that cannot be filtered out by the procedure described in sec. 2. Beamforming techniques based on static resp. rotating focus perform an implicit averaging over the rotor revolution and thereby, suppress these interfering frequency components to a certain degree, which will be shown next for comparison.

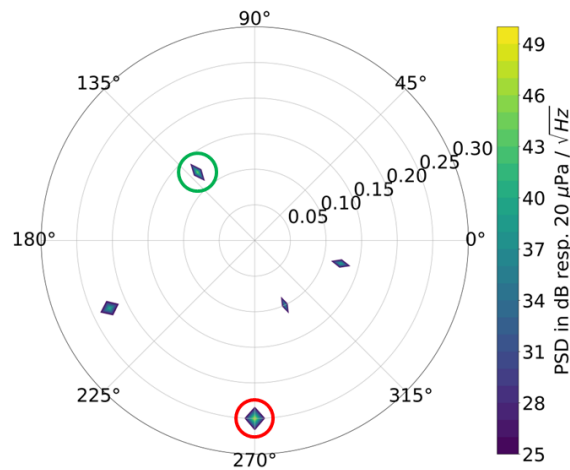


Figure 8: Source map for b11c test case evaluated at the trigger instant with analysis frequency of 2 kHz.

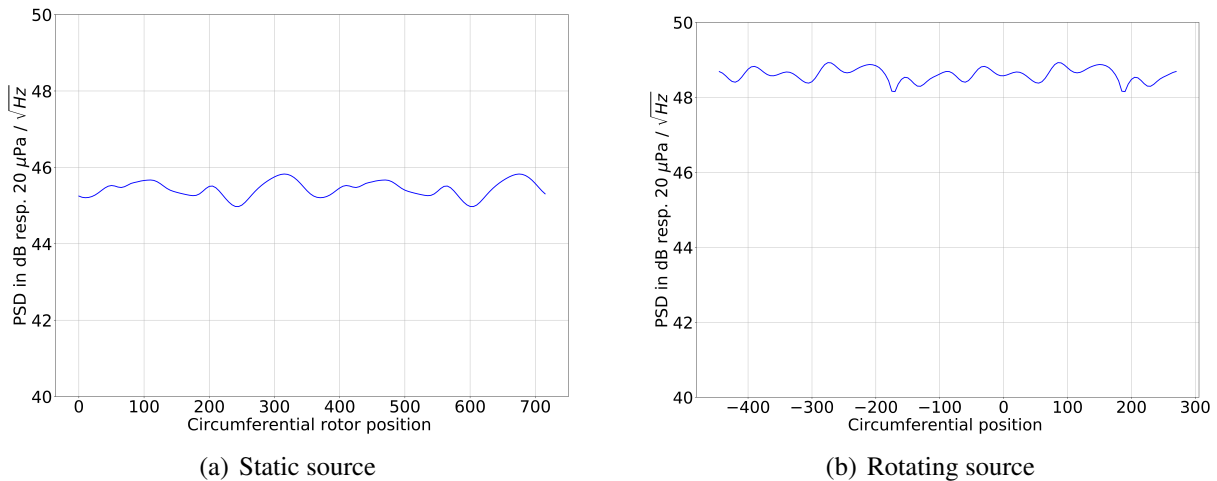


Figure 9: Instantaneous source levels at 2 kHz over two trigger intervals, i.e. two revolutions of the rotating source, for test case b11c with broadband source spectra.

Source localisation was performed with static and rotating focus separately. The static focus is based on the CSM of the fixed microphone data and the DAMAS deconvolution algorithm. The rotating focus utilises the signals of a virtual rotating array, which are obtained by Fourier-based interpolation in the azimuthal mode domain (cp. [15, 18]), for determination of the CSM. The results are shown in Fig. 10. Both methods identify the synthesised source of their respective motion type with good accuracy, i.e. a PSD of 43.4 dB for the static source using the static focus and a PSD of 48.0 dB for the rotating source using the virtual rotating array. The minimum level difference to the spurious sources is about 9 dB for the static focus and 13 dB for the rotating focus. Nevertheless, a larger number of spurious sources are visible for the analysis with separated focus compared to the instantaneous analysis shown in Fig. 8. These spurious sources are concentrated along the trajectory of the source that is out of focus.

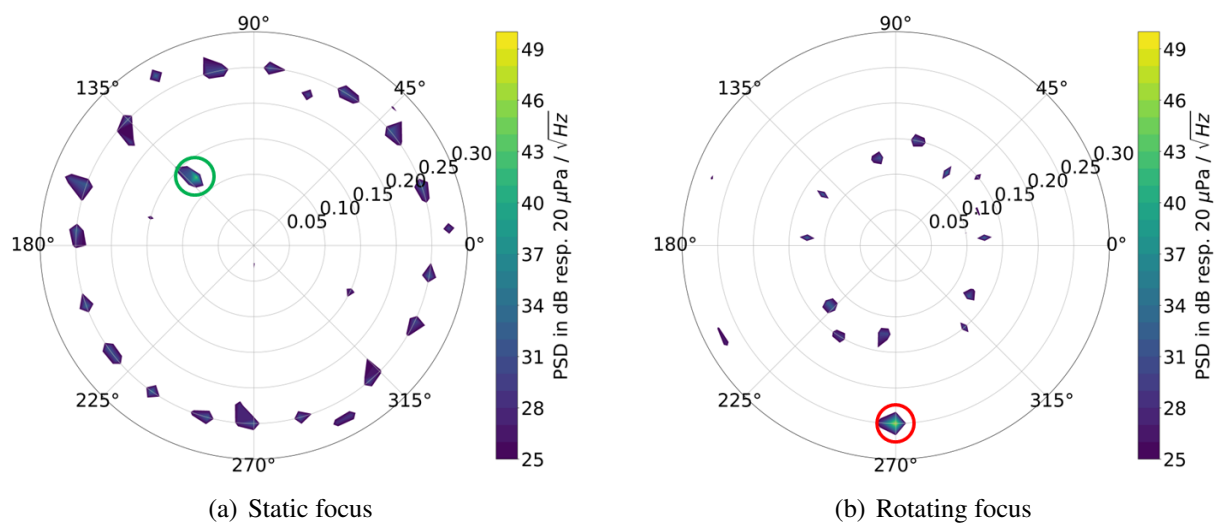


Figure 10: Source maps for b11c test case using static and rotating focus with analysis frequency of 2 kHz.

6 Conclusion

A new source localisation technique is presented that allows simultaneous separation of rotating and static sources by use of cyclostationary time-frequency analysis. The method enables the analysis of tonal and broadband source types basing on instantaneous spectra that provide the capability for source localisation over varying azimuthal rotor positions. Tests on simulated benchmark cases show that the method successfully detects the sources and their types of motion. Exact reconstruction of the source positions and strengths is verified for a test case with tonal source spectra. For broadband source spectra, the source levels are slightly overestimated, which is caused by interference from neighbouring frequency components. The comparison with Beamforming results for static and rotating focus show that the suppression of spurious sources by the instantaneous source localisation technique is reduced. Algorithmic improvements to increase the dynamic range of the source localisation will be part of further investigations as well as experimental validation using static and rotating loudspeaker arrays. The extension of the presented source localisation technique to analysing sources with rotor-dependent amplitude modulation by adaptation of the Wigner-Ville spectrum will provide deeper insight into the sound generation mechanisms at fan stages in presence of inflow distortion.

References

- [1] J. Antoni. “Cyclostationarity by examples.” *Mechanical Systems and Signal Processing*, 23, 987–1036, 2009.
- [2] D. Baron, M. B. Wakin, M. F. Duarte, S. Sarvotham, and R. G. Baraniuk. “Distributed compressed sensing.” 2005.
- [3] M. Behn, R. Kisler, and U. Tapken. “Efficient azimuthal mode analysis using compressed

- sensing.” In *22nd AIAA/CEAS Aeroacoustics Conference*. Lyon, France, 2016. AIAA 2016-3038.
- [4] M. Behn, B. Pardowitz, and U. Tapken. “Separation of tonal and broadband noise components by cyclostationary analysis of the modal sound field in a low-speed fan test rig.” In *fan2018*. Darmstadt, Germany, 2018. Paper-No. 043.
- [5] B. Boashash. “Note on the use of the wigner distribution for time-frequency signal analysis.” *IEEE Transactionas on Acoustics, Speech, and Signal Processing*, 36(9), 1518–1521, 1988.
- [6] T. F. Brooks and W. M. Humphreys, Jr. “A deconvolution approach for the mapping of acoustic sources (DAMAS) determined from phased microphone array.” *J. Sound Vib.*, 294(4-5), 856–879, 2006. doi:10.1016/j.jsv.2005.12.046.
- [7] W. Chen and X. Huang. “Wavelet-based beamforming for high-speed rotating acoustic source.” *IEEE Access*, 4, 2016.
- [8] R. P. Dougherty and B. E. Walker. “Virtual rotating microphone imaging of broadband fan noise.” In *15th AIAA/CEAS Aeroacoustics Conference*. Miami, Florida (USA), 2009. AIAA 2009-3121.
- [9] L. Grizewski, M. Behn, S. Funke, and H. Siller. “Analysis of the influence of inflow distortions on turbofan rotor noise.” In *25th AIAA/CEAS Aeroacoustics Conference*. Delft, Netherlands, 2019. AIAA 2019-2719.
- [10] Y.-H. Heo, J.-G. Ih, and H. Bodén. “Acoustic source identification of an axial fan in a duct considering the rotation effect.” *Journal of the Acoustical Society of America*, 140(1), 145–156, 2016.
- [11] G. Herold. “b11: Rotating Point Sources.” <https://www.b-tu.de/fg-akustik/lehre/aktuelles/arraybenchmark>, 2017.
- [12] G. Herold, C. Ocker, E. Sarradj, and W. Pannert. “A comparison of microphone array methods for the characterization of rotating sound sources.” In *7th Berlin Beamforming Conference*. Berlin, Deutschland, 2018. BeBeC-2018-D22.
- [13] G. Herold and E. Sarradj. “Microphone array method for the characterization of rotating sound sources in axial fans.” *Noise Control Engineering Journal*, 63(6), 546–551, 2015.
- [14] D. Kim and J. P. Haldar. “Greedy algorithms for nonnegativity-constrained simultaneous sparse recovery.” *Signal Processing*, 125, 274–289, 2016.
- [15] C. R. Lowis. *In-duct measurement techniques for the characterisation of broadband aer-engine noise*. Dissertation, University of Southampton, Southampton, UK, 2008.
- [16] P. Mo and W. Jiang. “A hybrid deconvolution approach to separate static and moving single-tone acoustic sources by phased microphone array measurements.” *Mechanical Systems and Signal Processing*, 84, 399–413, 2017.

- [17] A. Moreau. *A unified analytical approach for the acoustic conceptual design of fans of modern aero-engines*. Dissertation, Technische Universität Berlin, Berlin, Germany, 2017.
- [18] C. Ocker and W. Pannert. “Calculation of the cross spectral matrix with daniell’s method and application to acoustical beamforming.” *Applied Acoustics*, 120, 59–69, 2017.
- [19] M. A. Poletti. “Series expansions of rotating two and three dimensional sound fields.” *Journal of the Acoustical Society of America*, 128(6), 3363–3374, 2010.
- [20] E. Sarradj. “Three-Dimensional Acoustic Source Mapping with Different Beamforming Steering Vector Formulations.” *Advances in Acoustics and Vibration*, 2012, 2012. doi: 10.1155/2012/292695.
- [21] E. Sarradj and G. Herold. “A Python framework for microphone array data processing.” *Applied Acoustics*, 116, 50–58, 2017. doi:10.1016/j.apacoust.2016.09.015.
- [22] P. Sijtsma. “Location of rotating sources by phased array measurements.” research report NLR-TP-2001-135, NLR, 2001.
- [23] P. Sijtsma. “Circular harmonics beamforming with multiple rings of microphones.” research report NLR-TP-2012-247, NLR, 2012.
- [24] M. Staggat, A. Moreau, and S. Guérin. “Analytical prediction of boundary layer ingestion noise for an integrated turbofan.” In *Proceedings of the 26th International Congress on Sound and Vibration (ICSV)*. Montréal, Canada, 2019.
- [25] J. Tropp, A. Gilbert, and M. Strauss. “Simultaneous sparse approximation via greedy pursuit.” In *IEEE International Conference on Acoustics, Speech, and Signal Processing ICASSP’05*. Philadelphia, Pennsylvania (USA), 2005.